Relaxation to a Phase-Locked Equilibrium State in a One-Dimensional Bosonic Josephson Junction

Marine Pigneur,[1] Tarik Berrada,[1] Marie Bonneau,[1] Thorsten Schumm,[1] Eugene Demler,[2] and Jörg Schmiedmayer[1,*]
[1]Vienna Center for Quantum Science and Technology, Atominstitut, TU Wien, Stadionallee 2, 1020 Vienna, Austria
[2]Department of Physics, Harvard University, Cambridge, Massachusetts 02138, USA

(Received 17 November 2017; published 27 April 2018)

We present an experimental study on the nonequilibrium tunnel dynamics of two coupled one-dimensional Bose-Einstein quasicondensates deep in the Josephson regime. Josephson oscillations are initiated by splitting a single one-dimensional condensate and imprinting a relative phase between the superfluids. Regardless of the initial state and experimental parameters, the dynamics of the relative phase and atom number imbalance shows a relaxation to a phase-locked steady state. The latter is characterized by a high phase coherence and reduced fluctuations with respect to the initial state. We propose an empirical model based on the analogy with the anharmonic oscillator to describe the effect of various experimental parameters. A microscopic theory compatible with our observations is still missing.

DOI: 10.1103/PhysRevLett.120.173601

The recent experimental advances in manipulating and probing ultracold atomic gases established them as an ideal model system to study the nonequilibrium dynamics and relaxation of isolated quantum systems [1]. While a relaxation seems in contradiction with a unitary evolution, both theoretical and experimental works [1–3] show that nonintegrable systems reach a relaxed state resembling a Gibbs ensemble [4]. Integrable systems generally relax to prethermal steady states, for which a description by a generalized Gibbs ensemble reflects the conserved quantities in the system [1,5]. The thermalization of nearly integrable systems is of peculiar interest.

In this context, an interesting model system is a bosonic Josephson junction consisting of two coupled superfluids [6–10]. In reduced dimensions (1D), the physics can be essentially described by the quantum sine-Gordon model [11–15], as recently verified for systems in thermal equilibrium [16]. The dynamics occurring after a quench of the tunnel coupling was recently studied [17] and showed a slow relaxation saturating at a low phase coherence, see also related discussions [18,19]. In this Letter, we present an experimental study demonstrating a complete relaxation to a phase-locked equilibrium state.

Our experimental system consists of two one-dimensional quasicondensates (1D-BEC) of ^{87}Rb magnetically trapped in a double-well potential with tunable barrier height. The preparation protocol relies on an atom chip [20] to coherently manipulate the wave packets [21]. The various steps are illustrated in Fig. 1, together with experimental fluorescence pictures obtained after a time of flight of 46 ms [22].

We start the sequence with a single 1D-BEC of 750–4500 atoms in an elongated trap of frequencies $\omega_z = 2\pi \times 22$ Hz (longitudinally) and $\omega_{x,y} = 2\pi \times 3$ kHz (transversely) [Fig. 1(a)]. The largest chemical potential computed with [23] is $\mu = 2.4$ kHz. Yang-Yang thermometry [24] gives an estimate of the initial temperature of $T = 18(3)$ nK.

Using radio-frequency dressing [25,26], we deform the trap in 21.5 ms by continuously raising a barrier and obtain a double-well potential elongated along the z axis and symmetric with respect to the barrier [Fig. 1(b)]. The barrier is made high enough to neglect tunneling, such that the two 1D-BECs are considered decoupled. We define the relative phase as

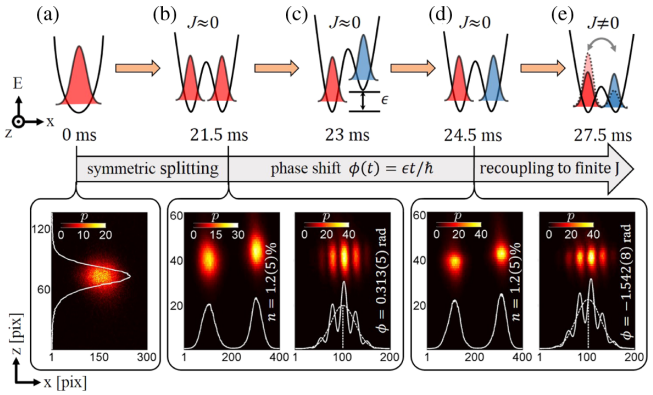

FIG. 1. Schematic of the preparation sequence consisting in a splitting (a,b) of the original wave packet to a decoupled trap, a phase imprinting between the wave packets (c,d), and a recoupling to initiate tunneling dynamics (e). The captions display the fluorescence pictures (averaged over 10 repetitions) of the atomic density after 46 ms time of flight and the corresponding integrated profiles.

$$\phi(t) = \phi_L(t) - \phi_R(t), \quad (1)$$

with $\phi_{L,R}(t)$ being the phase of the left and right component, respectively. The phase is experimentally extracted from the interference pattern resulting from the overlap of the wave functions after time of flight [cf. pictures in Figs. 1(b) and 1(d)]. The conjugated variable is the normalized atom number imbalance defined by

$$n(t) = \frac{N_L(t) - N_R(t)}{N_L(t) + N_R(t)}, \quad (2)$$

with $N_{L,R}(t)$ being the atom number of the left and right component, respectively. The imbalance measurement requires us to move the clouds further apart by raising the barrier height. This prevents their overlap in time of flight. At this stage, the averaged values of both the imbalance and the phase are close to zero [cf. pictures in Figs. 1(b) and 1(d)] due to the trap symmetry.

We then imprint a initial relative phase ϕ_0 by shifting one site of the double well along the vertical y axis in 1.5 ms [Fig. 1(c)]. This introduces an energy difference ϵ between the two sites and results in a phase accumulation $\phi(t) = \epsilon t/\hbar$. The trap symmetry is then re-established in 1.5 ms [Fig. 1(d)]. We prepare a relative phase between 0 and π by varying the value of the vertical shift. The phase appears as a shift between the integrated profile maximum and the center of the envelope, as displayed in the fluorescence pictures in Fig. 1(d) and Fig. 3(a). The straightness of the fringes shows that the relative phase is uniformly imprinted along the elongated direction of the condensate with negligible fluctuations at the scale of the imaging resolution (4 μm in object space) [22]. In the decoupled trap, the relative phase randomizes under the effect of interaction-induced phase diffusion [27–29]. In our case, this effect is strongly reduced by a large number-squeezing factor obtained by the splitting of the initial BEC [21,30]. We define the number-squeezing factor by $\xi_N = \Delta n/\sqrt{N}$, with Δn the standard deviation of the imbalance distribution and N the total atom number. For our typical atom number $N = 2500(200)$ atoms, we obtain $\xi_N = 0.57(6)$. The corresponding phase diffusion rate is $0.05(2)$ rad/ms. In circular statistics, the phase coherence is indicated by the phasor R of the phase distribution, which varies between 0 for a random distribution and 1 for a perfectly narrow one. The phasor degrades from $R_{\text{split}} = 0.94(2)$ after splitting to $R_0 = 0.91(2)$ at the end of the preparation sequence, indicating that a high phase coherence is preserved [Fig. 3(a)] and that the initial phase ϕ_0 is well defined. The imbalance is not affected by the phase shift such that its value is $n_0 \approx 0$.

Finally, the barrier is lowered in 3 ms [Fig. 1(e)]. This initiates a tunneling dynamics characterized by a single particle tunnel-coupling strength varying between $J/h = 2(1)$ Hz and $J/h = 32(3)$ Hz. The corresponding transverse frequencies vary between $\omega_x = 2\pi \times 1.2$ kHz and $\omega_x = 2\pi \times 1.5$ kHz. The chemical potential ranges from $\mu/h = 0.9$ kHz to $\mu/h = 1.4$ kHz and always remains lower than the next transverse excited state energy (in this case, the second excited state). We then neglect the population of atoms in higher transverse states.

We investigate the dynamics by destructively measuring the phase and imbalance alternatively to reconstruct the entire dynamics. A typical example of the oscillating dynamics is displayed in Fig. 2 for $N = 3300(600)$ atoms, $\phi_0 = -1.3(4)$ rad, and $n_0 = -0.004(13)$. The oscillations of the mean phase and imbalance present a damping on a timescale of 15 ms toward an equilibrium state ($n_{eq} \approx 0, \phi_{eq} \approx 0$) without decrease of the total atom number. While the oscillations are expected from a 2-mode Bose-Hubbard model [31], such a damping goes beyond the existing microscopic descriptions [17,18,32].

The analysis of the individual fluorescence images shows that the fringe patterns after damping are straight and centered on the envelope maximum, as displayed in

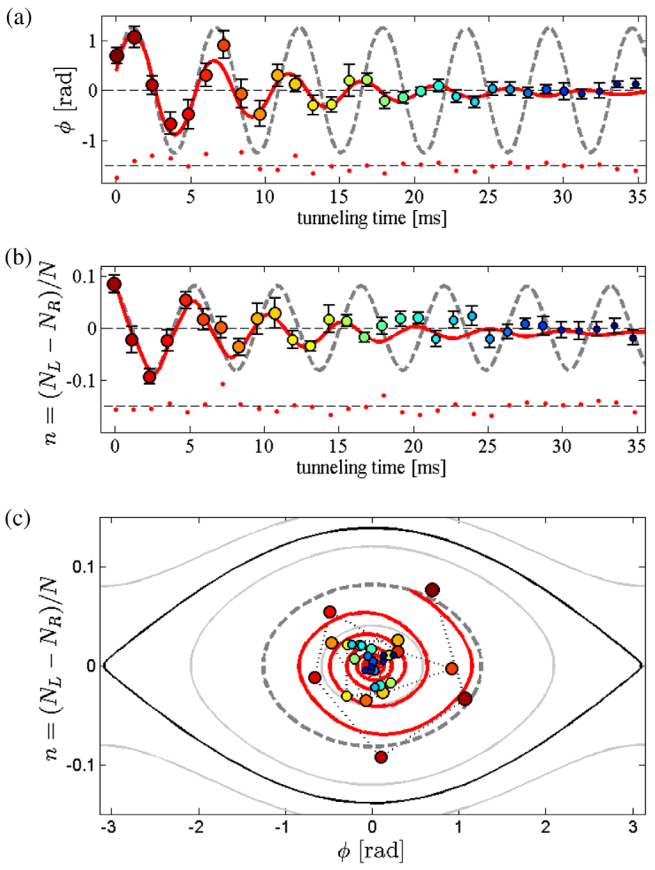

FIG. 2. Damped Josephson oscillations of the relative phase (a) and imbalance (b) for $N = 3300(600)$ atoms, $\phi_0 = -1.3(4)$ rad, and $n_0 = -0.004(13)$. Red line: fit result giving a damping time $\tau = 9.8(2)$ ms, $U/h = 0.71(15)$ Hz, and $J/h = 8(2)$ Hz. Red dots: residuals (shifted for clarity). Dashed line: corresponding predictions of the mean-field 2-mode Bose-Hubbard model. (c) Evolution in the phase portrait representation.

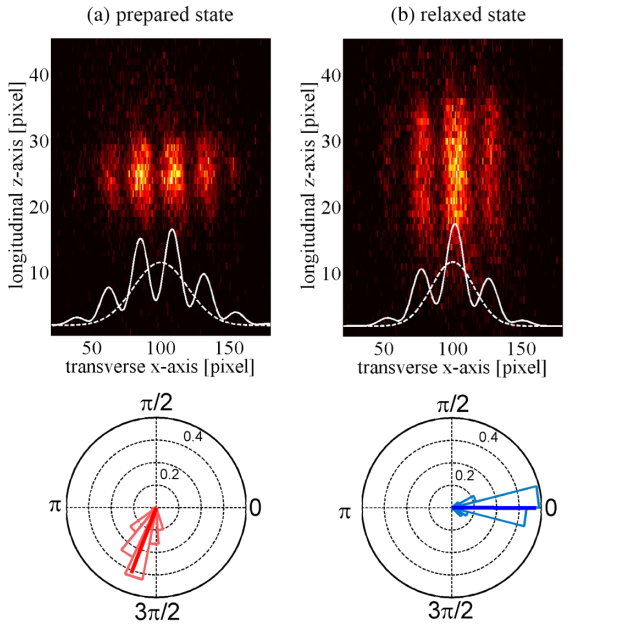

FIG. 3. (a) Top: interference fringes for the initial state obtained by fluorescence imaging and corresponding integrated density profile. Bottom: phase distribution (50 realizations) showing a high phase coherence. (b) Corresponding quantities after relaxation. We observe a uniform phase-locking without degradation of the phase coherence. A slow breathing mode is visible as an expansion of the fringes (see Supplemental Material [33]).

Fig. 3(b). We deduce that the relative phase reaches the value of zero uniformly along the condensate. Furthermore, the contrast of the integrated fringes barely degrades from $C_0 = 0.56(7)$ to $C_{\mathrm{eq}} = 0.49(8)$. This indicates that the longitudinal phase fluctuations do not increase at the timescale of the damping.

The phase distribution, obtained from 50 repetitions of an experimental sequence, shows that the phase locking is very reproducible [Fig. 3(b)]. After relaxation, the phasor value reaches $R_{\mathrm{eq}} = 0.96(2)$, corresponding to a coherence factor of $\langle \cos(\phi_{\mathrm{eq}}) \rangle = 0.95(2)$. The phase coherence reaches a value exceeding the theoretical expectation [17] and the relaxation dominates over the dephasing phenomena expected in such a system [34].

The relaxation is observed for a broad range of experimental parameters. In order to analyze the damped oscillations obtained under various conditions, we develop a phenomenological model adapted from the mean-field 2-mode Bose-Hubbard model [7]. We call U the on-site interaction energy and J the single particle tunnel-coupling energy. The ratio $NU/2J$ is in the order of 100, placing our experiment deeply into the Josephson regime [35]. The derivation of the Hamiltonian for a symmetric trap gives the following undamped time evolution of the phase and imbalance:

$$\dot{n}(t) \approx -\frac{2J}{\hbar}\sqrt{1-n^2(t)}\sin[\phi(t)], \tag{3}$$

$$\dot{\phi}(t) \approx \frac{NU}{\hbar}n(t) + \frac{2J}{\hbar}\frac{n(t)}{\sqrt{1-n^2(t)}}\cos[\phi(t)]. \tag{4}$$

The interplay between the interatomic interaction NU and the tunneling $2J$ leads to different dynamical modes. As demonstrated in [31], every state initialized with no imbalance results in Josephson oscillations of the phase and imbalance characterized by the plasma frequency $\omega_p \approx \sqrt{NU2J}/\hbar$. Our experimental protocol prepares $n(0) \approx 0$ to remain in the oscillating regime. The system presents an analogy with a classical momentum-shortened pendulum [36] in which the relative phase ϕ is analogous to the pendulum angle, and the imbalance n is proportional to its momentum $\dot{\phi}$. In [36], the length of the pendulum is defined by $l(t) = \sqrt{1-n^2(t)}$. Defining N_0 as the amplitude of the n oscillations, it follows from [31] that $N_0 \leq 2\sqrt{2J/NU}$ in the limit of $NU \gg 2J$. Consequently, the momentum shortening is negligible in our case, and the analytical solution of a rigid pendulum expressed in terms of the sn-Jacobi elliptic function is a good approximation [37,38]. To account for the damping of the oscillations, we follow the approach of [36] and add a dissipative term to Eq. (3):

$$\dot{n}(t) \approx -\frac{2J}{\hbar}\sqrt{1-n^2(t)}\sin[\phi(t)] - \frac{\eta}{N}\dot{\phi}(t), \tag{5}$$

where η is an empirical dimensionless viscosity. Here, η normalized by N has the physical meaning of the shunting conductance in the resistively and capacitively shunted junction model, in which a damping appears as in Eq. (5) [39,40]. The viscosity results in an exponential decay with the characteristic time τ. In the harmonic regime and in the limit $NU \gg 2J$, τ reads

$$\tau(U) \approx \frac{2\hbar}{U\eta}. \tag{6}$$

Assuming that Eq. (6) holds true for large amplitude oscillations, we empirically modify the analytical solutions to account for a damping. The phase $\phi(t)$ and the imbalance $n(t)$ become

$$\phi(t) \approx 2\arcsin\left[\sin\left(\frac{\Phi_0}{2}\right)e^{-t/\tau} \times \mathrm{sn}\left(\omega t + \phi' \middle| \sin\left(\frac{\Phi_0}{2}\right)e^{-t/\tau}\right)\right], \tag{7}$$

$$n(t) \approx \frac{N_0}{\omega \times 2\sin(\frac{\Phi_0}{2})}\dot{\phi}(t). \tag{8}$$

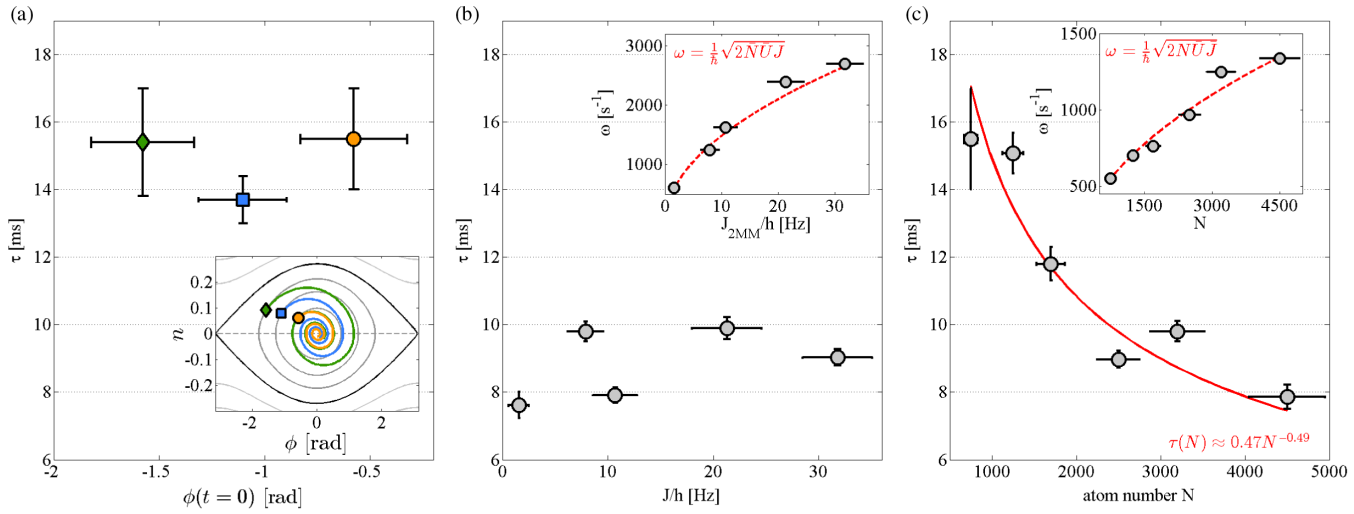

FIG. 4. Relaxation dependence on parameters. (a) Variation of τ with the initial phase for $N = 750(100)$ atoms and $J/h = 6(1)$ Hz. The damping time remains constant within the error bars, excluding a dependence on the oscillation amplitudes. Inset: fit results for the various prepared phases showing the self-consistency of the trajectories. (b) Variation of τ with the tunnel coupling for $N = 3500(500)$ atoms and $\phi_0 = 1.93(35)$ rad; τ does not present a dependence on the tunnel coupling J/h between 2(1) Hz and 32(3) Hz. Inset: fit results for the plasma frequency ω and prediction of the 2-mode model for constant values of $\bar{N} = 3500$ atoms and $\bar{U}/h = 0.85$ Hz (red dashed line). (c) Variation of τ with the atom number N for $J/h = 7(2)$ Hz and $\phi_0 = -1.48(98)$ rad; τ presents a dependence in $1/\sqrt{N}$ (red line). Inset: ω versus N and prediction of the 2-mode model (dashed red line) for the averaged values $\bar{U}/h = 0.71$ Hz and $\bar{J}/h = 7$ Hz deduced from the fit parameters.

Here, Φ_0 and N_0 are the amplitudes of the phase and imbalance oscillations, respectively, and ω is the damped harmonic frequency, which differs from the plasma frequency ω_p by $\omega = \sqrt{\omega_p^2 - 1/\tau^2}$. However, the correction introduced by τ is negligible. Also, ϕ' is a temporal shift of the oscillations to compensate that the sn-function conventionally starts at $\phi(0) = \Phi_0$. The argument $\sin(\Phi_0/2)e^{-t/\tau}$ in the sn-function describes the anharmonicity of the oscillation, initially set by Φ_0 and exponentially decreasing over time under the effect of η. We establish a connection between U, J, and η of the 2-mode model and N_0,Φ_0, ω, and τ of the pendulum analogy. It relies on the approximation $\omega \approx \omega_p$, on the definition of τ given by Eq. (6) and on the comparison of Eq. (8) with the linearized Eq. (4).

$$J \approx \frac{\hbar\omega}{4}\frac{N_0}{\sin(\Phi_0/2)}, \tag{9}$$

$$U \approx 2\hbar\omega\frac{\sin(\Phi_0/2)}{N \times N_0}, \tag{10}$$

$$\eta \approx \frac{N \times N_0}{\tau\omega\sin(\Phi_0/2)}. \tag{11}$$

We use Eqs. (7) and (8) as a fit model. The small amplitude of the n oscillations makes it difficult to estimate N_0. As η depends on N_0 through Eq. (11), fitting the dynamics with Eqs. (4) and (5) is unreliable. In contrast, τ shows no correlations with N_0 and indicates clearly the effect of the experimental parameters on the relaxation mechanism. We recover the values of U and J using Eqs. (9) and (10) and insert them in Eqs. (3) and (4) to build the phase portrait presented in Fig. 2(c) and in the inset of Fig. 4(a).

Equations (7) and (8) reproduce the decay of the oscillations amplitude. Also, as the system gets closer to the harmonic regime, the oscillation frequency increases. This is shown in Figs. 2(a) and 2(b) when comparing the data and fit (red line) with the undamped prediction (dashed gray line) of the 2-mode model. The absence of structure in the residuals shows that it is justified to fit the dynamics with a unique damping time, similarly to a pendulum evolving in a medium of fixed viscosity. This implies that the relaxation does not depend on the amplitude of the oscillation.

A more systematic check of the dependence of τ on the oscillation amplitude is performed by preparing oscillations of initial phase ϕ_0 varied between -0.2π and -0.8π. Here, J and N are kept constant with $J/h = 6(1)$ Hz (fit result) and $N = 750(100)$ atoms. Figure 4(a) displays the values of τ for the different initial phases, and the inset shows the trajectories deduced from the fit in the phase portrait representation. We observe a constant damping time $\tau = 15(1)$ ms, corresponding to $\eta = 26(7)$. Since a larger initial phase also implies a larger amplitude of the imbalance oscillation, we can state that the relaxation is independent of the n-oscillation amplitude.

We also check the influence of the tunnel coupling strength between $J/h = 2(1)$ Hz and $J/h = 32(3)$ Hz (fit result).

The initial state is characterized by $N=3500(500)$ atoms, $n_0=-0.004(13)$, $\phi_0=-1.93(35)$ rad, $C_0=0.53(7)$, and $R_0=0.94(3)$. The fit results for the plasma frequency ω are displayed in the inset of Fig. 4(b) and follows the prediction of the 2-mode model. Figure 4(b) shows that the damping does not present an obvious dependence on J. This implies that the damping does not result from the tunneling dynamics of the wave functions nor from excitations to higher transverse modes. Additionally, the absence of dependence of τ on Φ_0, N_0, and J shows that the relaxation does not depend on the plasma frequency, that we can write as $\omega=(4J/\hbar N_0)\sin(\Phi_0/2)$. This excludes a friction between the atoms and a thermal background gas as a cause for the damping.

In the following, we measure the dynamics for a total atom number varied between 750 and 4500 atoms to investigate the effect on the relaxation. The barrier height is kept identical, and the change of atom number has a negligible impact on the tunnel coupling which remains $J/h=7(2)$ Hz. The prepared phase is $\phi_0=-1.48(98)$ rad, associated to a contrast $C_0=0.55(7)$ and a phasor $R_0=0.81(3)$. The typical initial imbalance for the largest atom number is $n_0=0.006(47)$. The variation of τ with the atom number is displayed in Fig. 4(c). We fit τ by the function αN^{β}, with α and β being the fit parameters, and obtain $\alpha=0.47(2)$ and $\beta=-0.49(3)$. According to Eq. (6), $\tau\propto 1/U\eta$, leading to $U\eta\propto\sqrt{N}$. The dependence of the viscosity η with the atom number depends on the variation of U with N.

In conclusion, we observe that the oscillating tunneling dynamics in a 1D bosonic Josephson junction relaxes to a phase-locked steady state. The timescale of the phenomenon remains unaffected by the amplitude and frequency of the oscillations. It is unchanged for a tunnel coupling J/h between 2 and 32 Hz and presents a dependence in approximately $1/\sqrt{N}$ with the atom number. The observed phase locking is much faster than predicted in [17–19] and leads to an equilibrium state with small fluctuations in phase and atom number imbalance. This questions the suitability of the quantum sine-Gordon model to describe the out-of-equilibrium tunneling dynamics of two 1D superfluids confined in a harmonic potential. Ongoing work aims at determining the microscopic origin of the relaxation. We attempt various theoretical approaches, including quenches in the sine-Gordon model using exact solutions in the single mode approximation, truncated Wigner approximation, and variational Gaussian approach. None of these reproduces the fast and complete phase locking we observe. A better understanding of the relaxation requires a study of the relaxed state and an estimation of its energy. While this could, in principle, be deduced from $J\langle\cos\phi\rangle$ and from the final phase fluctuations, the latter are dominated by our imaging resolution and imaging shot noise in the current experiment.

We are grateful to I. Mazets, T. Schweigler, G. Zaránd, I. Lovas, and E. Dalla Torre for helpful discussions and theoretical support. This research was supported by the ERC Advanced Grant QuantumRelax and by the Austrian Science Fund through the project SFB FoQuS (SFB F40). M. P. and T. B. acknowledge the support of the Doctoral Program CoQuS. M. B. was supported by a MC fellowship ETAB under Grant Agreement No. 656530. E. D. acknowledges the support of the Harvard-MIT CUA, NSF Grant No. DMR-1308435 and of the AFOSR Quantum Simulation MURI, AFOSR Grant No. FA9550-16-1-0323.

*schmiedmayer@atomchip.org

[1] T. Langen, R. Geiger, and J. Schmiedmayer, Annu. Rev. Condens. Matter Phys. **6**, 201 (2015).
[2] A. Polkovnikov and A. Silva, Rev. Mod. Phys. **83**, 863 (2011).
[3] J. Eisert, M. Friesdorf, and C. Gogolin, Nat. Phys. **11**, 124 (2015).
[4] M. Gring, M. Kuhnert, T. Langen, T. Kitagawa, B. Rauer, M. Schreitl, D. A. Smith, E. Demler, and J. Schmiedmayer, Sci. Rep. **337**, 1318 (2012).
[5] M. Rigol, V. Dunjko, V. Yurovsky, and M. Olshanii, Phys. Rev. Lett. **98**, 050405 (2007).
[6] M. Albiez, R. Gati, J. Fölling, S. Hunsmann, M. Cristiani, and M. K. Oberthaler, Phys. Rev. Lett. **95**, 010402 (2005).
[7] R. Gati and M. Oberthaler, J. Phys. B **40**, R61 (2007).
[8] S. Levy, E. Lahoud, I. Shomroni, and J. Steinhauer, Nature (London) **449**, 579 (2007).
[9] L. J. LeBlanc, A. B. Bardon, J. McKeever, M. H. T. Extavour, D. Jervis, J. H. Thywissen, F. Piazza, and A. Smerzi, Phys. Rev. Lett. **106**, 025302 (2011).
[10] G. Spagnolli, G. Semeghini, L. Masi, G. Ferioli, A. Trenkwalder, S. Coop, M. Landini, L. Pezze, G. Modugno, M. Inguscio, A. Smerzi, and M. Fattori, Phys. Rev. Lett. **118**, 230403 (2017).
[11] V. Gritsev, A. Polkovnikov, and E. Demler, Phys. Rev. B **75**, 174511 (2007).
[12] S. Coleman, Phys. Rev. D **11**, 2088 (1975).
[13] S. Mandelstam, Phys. Rev. D **11**, 3026 (1975).
[14] L. D. Faddeev and V. E. Korepin, Phys. Rep. **42**, 1 (1978).
[15] E. K. Sklyanin, L. A. Takhtadzhyan, and L. D. Faddeev, Theor. Math. Phys. **40**, 688 (1979).
[16] T. Schweigler, V. Kasper, S. Erne, I. E. Mazets, B. Rauer, F. Cataldini, T. Langen, T. Gasenzer, J. Berges, and J. Schmiedmayer, Nature (London) **545**, 323 (2017).
[17] E. G. DallaTorre, E. Demler, and A. Polkovnikov, Phys. Rev. Lett. **110**, 090404 (2013).
[18] L. Foini and T. Giamarchi, Phys. Rev. A **91**, 023627 (2015).
[19] L. Foini and T. Giamarchi, Eur. Phys. J. Spec. Top. **226**, 2763 (2017).
[20] M. Trinker, S. Groth, S. Haslinger, S. Manz, T. Betz, S. Schneider, I. Bar-Joseph, T. Schumm, and J. Schmiedmayer, Appl. Phys. Lett. **92**, 254102 (2008).
[21] T. Berrada, S. van Frank, R. Bücker, T. Schumm, J.-F. Schaff, and J. Schmiedmayer, Nat. Commun. **4**, 2077 (2013).
[22] R. Bücker, A. Perrin, S. Manz, T. Betz, C. Koller, T. Plisson, J. Rottmann, T. Schumm, and J. Schmiedmayer, New J. Phys. **11**, 103039 (2009).

[23] F. Gerbier, Europhys. Lett. **66**, 771 (2004).
[24] M. J. Davis, P. B. Blakie, A. H. van Amerongen, N. J. van Druten, and K. V. Kheruntsyan, Phys. Rev. A **85**, 031604 (2012).
[25] I. Lesanovsky, T. Schumm, S. Hofferberth, L. M. Andersson, P. Kruger, and J. Schmiedmayer, Phys. Rev. A **73**, 033619 (2006).
[26] S. Hofferberth, I. Lesanovsky, B. Fischer, J. Verdu, and J. Schmiedmayer, Nat. Phys. **2**, 710 (2006).
[27] M. Lewenstein and L. You, Phys. Rev. Lett. **77**, 3489 (1996).
[28] J. Javanainen and M. Wilkens, Phys. Rev. Lett. **78**, 4675 (1997).
[29] A. J. Leggett and F. Sols, Phys. Rev. Lett. **81**, 1344 (1998).
[30] G. B. Jo, Y. Shin, S. Will, T. A. Pasquini, M. Saba, W. Ketterle, D. E. Pritchard, M. Vengalattore, and M. Prentiss, Phys. Rev. Lett. **98**, 030407 (2007).
[31] S. Raghavan, A. Smerzi, S. Fantoni, and S. R. Shenoy, Phys. Rev. A **59**, 620 (1999).
[32] K. Sakmann, A. I. Streltsov, O. E. Alon, and L. S. Cederbaum, Phys. Rev. Lett. **103**, 220601 (2009).
[33] See Supplemental Material at http://link.aps.org/supplemental/10.1103/PhysRevLett.120.173601 for experimental preparation of the tunneling dynamics, paragraph "Splitting".
[34] I. Bouchoule, Eur. Phys. J. D **35**, 147 (2005).
[35] A. J. Leggett, Rev. Mod. Phys. **73**, 307 (2001).
[36] I. Marino, S. Raghavan, S. Fantoni, S. R. Shenoy, and A. Smerzi, Phys. Rev. A **60**, 487 (1999).
[37] K. Ochs, Eur. J. Phys. **32**, 479 (2011).
[38] L. Milne-Thomson, M. Abramowitz, and I. Stegun, Handbook of Mathematical Functions (United States Department of Commerce and National Bureau of Standards, Washington, D.C., 1972).
[39] M. Tinkham, *Introduction to Superconductivity* (McGraw-Hill, New York, 1975).
[40] G. Schön and A. Zaikin, Phys. Rep. **198**, 237 (1990).